

Title	Environmentally degradable, high-performance thermoplastics from phenolic phytomonomers
Author(s)	Kaneko, Tatsuo; Tran, Hang Thi; Shi, Dong Jian; Akashi, Mitsuru
Citation	Nature materials, 5(12): 966-970
Issue Date	2006-12
Type	Journal Article
Text version	author
URL	http://hdl.handle.net/10119/4959
Rights	This is the author's version of the work. Copyright (C) 2006 Nature Publishing Group. Tatsuo Kaneko, Tran Hang Thi, Dong Jian Shi & Mitsuru Akashi, Nature materials, 5(12), 2006, 966-970. http://dx.doi.org/10.1038/nmat1778
Description	

Environmentally-Degradable, High-Performance Thermoplastics from Multifunctional Phenolic Phytomonomers

Tatsuo Kaneko,^{1,2*} Hang Thi Tran,¹ Dong Jian Shi,¹ Mitsuru Akashi^{1*}

¹Department of Applied Chemistry, Graduate School of Engineering, Osaka University,
2-1, Yamadaoka, Suita, 565-0871, Japan.

²School of Materials Science, Japan Advanced Institute of Science and Technology,
1-1, Asahidai, Nomi, 923-1292, Japan.

*e-mail: kaneko@jaist.ac.jp

Aliphatic polyesters that degrade by hydrolysis, from naturally-occurring molecules form the main components of green plastics, which can be degraded into natural molecules¹. However, it was estimated that these polyesters become substitutes for only small percentage of currently-used nondegradable plastics since the application of the aliphatic polyesters such as poly(lactic acid), PLA, has been limited due to their too low thermal and mechanical properties to apply to an engineering plastic. Then, high-performance engineering plastics degrading into natural molecules are earnestly desired in human life. Although the use of a high-strength filler such as a bacterial cellulose² and modified lignin³ fantastically increases the plastic properties, the matrix polymers determine the intrinsic composite performance. The introduction of aromatic component into the thermoplastic polymer backbone is an efficient method to intrinsically improve the material performance^{3,4}. Here, we report the preparation of environmentally-degradable, liquid crystalline (LC), wholly-aromatic polyesters with performance as high as an engineering plastic. The polyesters were derived from polymerizable phytochemicals – in other words, “phytomonomers” widely present as lignin biosynthetic precursors⁵.

The phenolic phytochemical family with *p*-coumaryloyl group has a photosensitive phenylenevinylene and a polymerizable hydroxycarboxylic acid group, such as *p*-coumaric acid (4-hydroxycinnamic acid; 4HCA), ferulic acid (3-methoxy-4-hydroxycinnamic acid; MHCA), and caffeic acid (3,4-dihydroxycinnamic acid; DHCA). These molecules are widely available in various plants with an essential pathway of lignin biosynthesis⁵ and in several photosynthetic bacteria as one of the protein components⁶. Furthermore since their enzymatic synthetic roots from amino acids were well-defined to be very simple⁷, it is possible to perform the mass production of these phytomonomers. These phytomonomers were biodegraded by microbial action⁸. We have already prepared poly4HCA, which shows LC properties⁹. Although the LC polymers generally showed high mechanical strength for engineering use owing to the molecular orientation⁴, poly4HCA was very brittle due to its low molecular weight⁹ which has a high advantage of smooth degradation. However the high molecular weight poly4HCA were highly crystallized and exhibited no LC phase¹⁰. Then we tried to polymerize other phenolic phytomonomers MHCA and DHCA by the polycondensation procedure. Both polyMHCA and polyDHCA were not liquid crystalline or crystalline, and showed low mechanical strength. Flory showed theoretically that the polymerization of AB₂ type multifunctional monomers such as DHCA with one functional group (A) of one kind and two groups (B) of another kind created a hyperbranch architecture without cross-linkage¹¹ and later several researchers demonstrated this experimentally¹². PolyDHCA actually dissolved in dimethylformamide (DMF), suggesting the formation of not cross-linking but a hyper-branching architecture like lignin. The hyperbranch architecture with low-molecular-weight arms may cope with both **the degradability from the chain ends** and high mechanical performance. Therefore, we attempted to prepare hyper-branching LC polyarylates by the copolymerization of 4HCA with DHCA. As shown in Fig. 1a, the DHCA units can take the role of a branching point, and the oligo4HCA arms are rigid enough to show a LC phase. According to a semi-empirical calculation of model compounds for di(acetylcoumaryloyl) DHCA and di(acetylcoumaryloylcoumaryloyl) DHCA, the steric energy of the coumaryloyl esters ortho-locating to DHCA is not very high, and the propagation of the 4HCA arms is advantageous energetically (see Supplementary Information, Fig. S1). ¹H NMR spectroscopy in a mixed solvent of trifluoroacetic acid-*d*/dichloromethane-*d*₂

(1/5 v/v) demonstrated that the incorporation of both monomers into the polymer backbone and the copolymer composition, $C = \frac{[DHCA]}{[DHCA] + [4HCA]}$, can be estimated by the integration ratio of the aromatic proton signals of the individual units, and these results were summarized in Table 1. The C value was close to the monomer composition in the feed. The molecular weights of the copolymers were estimated by gel permeation chromatography (GPC). Although the number- and weight-average molecular weight ranged between $M_n = 1.8 \times 10^4 - 3.3 \times 10^4$ and $M_w = 4.4 \times 10^4 - 9.1 \times 10^4$, respectively. The polydispersity, M_n/M_w , ranged between 1.6-2.8 although the acetone-soluble fractions ($M_w < 5$ kDa) showed small values of M_n/M_w (< 1.3). All of the copolymers were soluble in aprotic polar solvents such as DMF (see Supplementary Information, Table S1), thus denying the cross-linked network formation. The high M_n/M_w values may be due to the hyper-branching architecture illustrated in Fig. 1a. X-ray diffraction studies showed that DHCA incorporation effectively reduced the degree of crystallization from 91 % to 0 %, as shown in Table 1 (XRD diagrams; see Supplementary Information, Fig. S2), presumably due to the hyperbranching architecture. If the poly(4HCA-co-DHCA)s were heated, they melted at specific temperatures to exhibit a thermotropic LC phase, where the Schlieren texture typical of a nematic state was observed by crossed-polarizing microscopy (Fig. 1b). The melting temperatures (T_m) were higher than 220 °C and the glass transition temperatures (T_g) ranged between 115-169 °C, which were much higher than the values of degradable bio-based polymers reported so far¹³ and high enough for engineering use { T_g of poly(bisphenol A carbonate), PC, is 145°C¹⁴} as shown in Table 1. Further heating induced a LC-crystal transition, which was characteristic of a poly4HCA homopolymer⁹. In the LC state, the samples behaved like a very soft elastomer, presumably due to chain entanglement enhanced by the hyper-branching architecture¹⁵. The copolymers were successfully processed in the nematic state into various shapes (Fig. 1c) by pressure application in molds, or by casting from a trifluoroacetic acid /dichloromethane (1/5 v/v) solution onto a Teflon-sprayed glass plate. In the nematic state, the samples were easily elongated by a pair of tweezers, and then cooled while maintaining the strain to form the stiff rectangles shown in the photo inset of Fig. 1d. Representative XRD image of the rectangles ($C = 38$ %) showed two broad diffraction spots at $2\theta = 19-21^\circ$ (θ : diffraction angle) corresponding to the spacing of

0.42-0.47 nm on the equatorial line, and four diffraction arcs at $2\theta=12.9^\circ$ corresponding to the spacing of 0.69 nm and at $2\theta=22.5^\circ$ corresponding to the spacing of 0.40 nm on the vertical line, as shown in Fig. 1d. The XRD pattern was typical of the nematic, and demonstrated an orientation at the molecular chain level. The diffractions on the equatorial line were assigned to random locations of the chains oriented along the fiber axis, whereas the diffractions on the vertical line might correspond to the length of the repeating units (0.8 nm). The orientation degree ranged between 0.52-0.58, which is relatively low as compared to other LCPs, presumably due to the hyper-branching architecture. A mechanical bending test of the oriented samples was performed (see Supplementary Information, Fig. S3). Table 1 shows the mechanical strength, σ , Young's modulus, E, and maximal strain, ε , ranging between 25-63 MPa, 7.6-16 GPa, and 1.2-1.3 respectively. σ values of the poly(4HCA-co-DHCA)s with C=25-50 mol% were comparable to those of PC¹⁴ and all the conventional environmentally-degradable polymers reported so far¹³ and E were much higher than them.

The hydrolytic behavior of the copolymers was investigated by an acceleration test in an alkaline buffer of pH=10 at 60 °C. Fig. 2a shows the time course of the weight change for the samples. The copolymers with a C of 45 % or lower showed a slight weight loss of at most 19 % of the initial weight to demonstrate the high durability. On the other hand, the copolymers with a C of 77 % and the DHCA homopolymer showed a rapid weight loss, with a half-life of about 15 days. The ¹H NMR spectra of the supernatant solution showed the signals at chemical shifts similar with the original polymers and the very tiny signals of monomers, and the peaks became much sharper than those of original polymers (see Supplementary Information, Fig. S6). Besides GPC of the supernatant solution showed only a peak at a maximum of Mn=2000 and high-performance liquid chromatography showed monomer peaks (retention time, RT: 15.562min, λ_{\max} : 225 and 310 nm) together with other peak presumably assigned to oligomers (RT: 16.063min, λ_{\max} : 225, 297 and 310 nm). This result indicates that the weight loss was due to the hydrolytic degradation and the circular pellets transformed into an amorphous shape accompanied with degradation. An increase in the DHCA composition enhanced the hydrolysis speed, presumably due to the decreased crystallization degree and the

enhanced **degradation from the chain ends** by hyper-branching architecture. Since the copolymer with a C of 77 % showed not only high values for the mechanical properties and thermotropic temperatures, but also hydrolytic degradability with a short half-life, it can be regarded as a hydrolytic engineering polymer that can be degraded into the original phytomolecules. Furthermore, some of the copolymer rectangles buried in soil for 10 months showed deformation (left photo of Fig. 2b and Fig. S7 in Supplementary Information) and an 8-13 % weight loss while PC co-buried with the copolymers in soil did not show deformation nor weight loss. Moreover, scanning electron microscopic (SEM) photo of the deformed poly(4HCA-co-DHCA) samples demonstrates that the existence of many holes with a diameter of about 10 μ m, contrast with the smooth surface of a hydrolytically-degraded compact (right photo), while co-buried PC showed a flat surface without holes. These findings can mean an environmental degradation of the copolymer compacts by natural functions not only rainwater but also microorganism action.

Fig. 3 shows the photoreactivity of the poly(4HCA-co-DHCA) copolymers. The time course of the photoreaction conversion monitored by UV-visible absorption spectroscopy of the copolymer thin-film cast onto quartz are shown in Fig. 3a. The absorption with a maximal peak at λ_{max} of 310 nm was reduced upon increasing the time of UV-irradiation. In contrast, the absorption ($\lambda_{\text{max}}=225$ nm) over the range of less than 250 nm increased by UV-irradiation, resulting in the appearance of an isosbestic point at $\lambda=250$ nm. UV-irradiation for more than 20 seconds made the copolymers insoluble in the solvent. We performed a ^1H NMR study of the soluble copolymers UV-irradiated for 10 seconds (Fig. 3b, C=45). Small signals appeared in the chemical shift range of 3.8-4.5 ppm upon UV-irradiation, supporting the formation of an aliphatic group substituted by the benzene ring or carbonyls. Infrared (IR) spectroscopy showed the decrement of the IR peaks for the double bonds and a shift of the carbonyl peak (see Supporting Information, Fig. S4). According to the literature, the photoreaction shown in Fig. 3c preferentially occurs in cinnamate molecules¹⁶. From these spectroscopic studies, it was demonstrated that UV-irradiation of the copolymers at ambient temperature induced a [2+2] cycloaddition of the vinylene units, forming the cyclobutane cross-linkage in the polymeric

chains (Fig. 3c). The photoreaction degree, as estimated by the absorption percent to the initial state, was plotted against the UV-irradiation time in Fig. 3d, showing a concave curve. The photoreaction speed was facilitated in the nematic state, similar to the poly4HCA photoreaction⁹ (see Supporting Information, Fig. S5). The photoreaction effects on the mechanical properties were investigated (Table 1). σ and E values were both increased up to maximum values of 104 MPa and 19 GPa, respectively, by the photoreaction, presumably due to the cross-linkage formation while ϵ value changes were negligible. On the other hand, the thermotropic temperatures were maintained regardless of the photoreaction. The effects of photoconversion from aromatic into aliphatic carboxyester on the hydrolysis were investigated. Samples UV-irradiated for 3 hours at ambient temperature were immersed in an alkaline buffer (n=2). **The UV-irradiated copolymers became insoluble in DMF and the supernatant showed no lower Mn peak in GPC, suggesting the cross-linkage formation and no UV-scission.** Fig. 2c shows the weight change in UV-irradiated copolymer pellets with various C values as a function of the degradation time. The C=45 % copolymer showed a shortening of the degradation half-life from more than 30 days to only 12 days following UV-treatment. The copolymers with C of 77 % and 100 % showed a very short half-life of 5 days. Furthermore, the UV-irradiation period controlled the hydrolysis speed (see Supporting Information, Fig. S8). The cyclobutane formation can attenuate the ester carbonyl conjugation with the phenylenevinylene to make it more polar and easier to **degrade randomly** and the cross-linking hardly affects the **degradation from the chain ends** (Fig. 2d). Since the λ_{\max} of the UV absorption peak of the copolymer was 310nm (UV-B), which is barely present in sunlight reaching on the ground atmosphere, the hydrolysis was not accelerated spontaneously. GPC of the cross-linked oligomers in the supernatant for 30 days degradation following UV-irradiation showed the peak of M_n =ca. 8000 higher than M_n (<2000) of the linear oligomers from not-UV-irradiated polymers. However, post UV-irradiation (λ =254 nm, 20 hours) to the cross-linked oligomers supernatant showed a peak-shift to M_n <1000 as a result of inverse cyclobutane-vinylene photoconversion¹⁷.

Thus, we successfully prepared a high-performance green polymers, poly(4HCA-co-DHCA)s, with

photo-tunable hydrolytic properties can lead to develop novel, environmentally-circulating engineering plastics for the automobile, aircrafts, electronic device and other materials. We finally propose that the positive use of AB_x-type multifunctional phytomonomers widely exist as amino acids, glycolipids, and other metabolites will take the new turn of high-functional and high-performance green polyesters or polyamides with the hyperbranch architecture.

References and Notes

- 1) Stevens, E. S. Green Plastics: An introduction to the new science of biodegradable plastics. (Princeton University Press, New Jersey, 2002).
- 2) Yano H. *et al.* Optically transparent composites reinforced with networks of bacterial nanofibers. *Adv. Mater.* **17**, 153-155 (2005).
- 3) Thielemans, W. & Wool, R. Lignin esters for use in unsaturated thermosets: lignin modification and solubility modeling. *Biomacromolecules* **6**, 1895-1905 (2005).
- 4) Madhavamoorthi, P. VECTRA liquid crystal polymer fiber. *Synthetic Fibers* **33**, 16-28 (2004).
- 5) Ricarda N., Anthony J. M. & Cathie M. Engineering plants with increased levels of the antioxidant chlorogenic acid. *Nat. Biotechnol.* **22**, 746-754 (2004).
- 6) Kyndt J.A., Meyer T. E., Cusanovich M. A. & Van Beeumen J. J., Characterization of a bacterial tyrosine ammonia lyase, a biosynthetic enzyme for the photoactive yellow protein *FEBS Lett.* **512**, 240 (2002).
- 7) Boerjan W., Ralph J. & Baucher M. Lignin biosynthesis *Annu. Rev. Plant Biol.* **54**, 519-546 (2003).
- 8) Cain R. B., Bilton R. F. & Darrah J. A. The metabolism of aromatic acids by micro-organisms. Methanolic pathways in the fungi. *Biochem. J.* **108**, 797-828 (1968)
- 9) Kaneko T., Matsusaki M., Hang T. T. & Akashi M. Thermotropic liquid crystalline polymer derived from natural cinnamoyl biomonomers. *Macromol. Rapid Commun.* **25**, 673-677 (2004).
- 10) Tanaka Y. *et al.* Solid-state polycondensation of p-hydroxy-*trans*-cinnamic acid under high pressure *Polym. Lett. Ed.* **13**, 235-242 (1975).
- 11) Flory, P. J. Molecular size distribution in three dimensional polymers. VI. Branched polymers containing A-R-B_{f-1} type units. *J. Am. Chem. Soc.* **74**, 2718-2723 (1952).
- 12) For example, Kricheldorf, H. R. & Stoeber, O. New polymer syntheses, 76. Hyperbranched polyesters by polycondensation of silylated 5-acetoxyisophthalic acid. *Macromol. Rapid Commun.* **15**, 87-93 (1994).
- 13) For example, Gross R. A. & Kalra B. Biodegradable polymers for the environment *Science*, **297**, 803-807 (2002).
- 14) Pochan, J. M. & Pochan, D. F. Dielectric relaxation studies of bis[4-(diethylamino)-2-methylphenyl]

phenylmethane/polycarbonate solid solutions. A correlation of sub-T_g relaxations and the glass transition activation energy *Macromolecules* **13**, 1577-1582 (1980).

- 15) Weng, W., Markel, E. J. & Dekmezian, A. H. Synthesis of long-chain branched propylene polymers via macromonomer incorporation. *Macromol. Rapid Commun.* **22**, 1488-1492, (2001).
- 16) Maekawa, Y. *et al.* Radiation-induced reactions via the lowest excited states in cinnamic acid crystals. *Chem. Commun.* 2088-2089 (2002).
- 17) Lendlein, A., Jiang H., Juenger, O. & Langer, R. Light-induced shape-memory polymers. *Nature* **434**, 879-882 (2005).

Acknowledgements

This research was supported mainly by a Grant-in-Aid for NEDO (03A44014c) and Handai FRC. TK thanks to Prof. K. Hirata, Y. Nagase, T. Bamba, and M. Kaneko (Osaka Univ.) for helpful discussion about bioproduction of phytomonomers and in-soil degradation, to Dr. Yoshida (Wako Chemical Co. Ltd) for his help in measuring HPLC, and to Dr. K. Hasegawa and J. Kadota (Osaka Municipal Tech. Res. Inst.) for their help in material processing. Correspondence and requests for materials should be addressed to T.K. Supplementary Information accompanies the paper on www.nature.com/naturematerials

Competing interests statement

The authors declare that they have no competing financial interests.

Table 1. Synthetic conditions of poly(4HCA-co-DHCA)s, and their performance.^a

polymers ^b	Mw	Mn/Mw	C in copolymer ^c	Yield	Degree of crystallization ^d	σ^e	E ^e	ε^e	Tg ^f	Tm ^f	T ₁₀ ^g	Biodegradability ^h
(mol%)	(x10 ⁴)		(mol%)	(wt%)	(%)	(MPa)	(GPa)		(°C)	(°C)	(°C)	
0	i	i	0	84	91	X	X	X	N	220	300	slow
25	4.4	2.4	21	80	38	38(64)	11(17)	1.3	169	225	290	slow (fast)
40	4.8	1.6	38	79	10	63(88)	11(15)	1.3	157	250	305	slow (fast)
50	9.1	2.8	45	80	9	50(104)	16(19)	1.2	124	260	310	medium (fast)
75	8.0	2.6	77	79	0	25(29)	7.6(9.2)	1.2	115	220	315	fast
100	7.0	2.4	100	69	0	X	X	X	114	N	320	fast
PHB	-	-	-	-	-	40	4.0	-	-12	177	-	fast
PCL	-	-	-	-	-	24	0.27	-	-60	57-60	-	fast
PLA	-	-	-	-	-	68	2.1	-	55	149	-	fast
PC	-	-	-	-	-	55	2.0	-	157	225	-	none

a) The copolymerization of *p*-coumaric acid (4-hydroxycinnamic acid; 4HCA) with caffeic acid (3,4-dihydroxycinnamic acid; DHCA) was carried out in the presence of acetic anhydride and sodium acetate with mechanical stirring for 6 hours at 200 °C. b) Numerals refer to the molar percentage of in-feed composition, C, of the DHCA units in poly(4HCA-co-DHCA)s. PHB refers to polyhydroxybutyrate (Biopole™). PCL refers to poly(ϵ -caprolactone). PLA refers to poly(lactic acid). PC refers to poly(bisphenol A carbonate)¹⁴. The data were originated from polymer database <http://polymer.nims.go.jp>. c) The C values in copolymers were measured from aromatic proton signals by ¹H NMR spectroscopy. d) The degree of crystallization was measured from the X-ray diffraction diagram. e) The mechanical properties were measured by a stress-strain bending test. The abbreviations “ σ ” “E”, and “ ε ” refer to mechanical strength, Young’s modulus, and maximal strain, respectively. The data in parenthesis were obtained after UV-irradiation for 4 hours (wavelength: >250nm, strength: 130 mW•cm⁻²). Error distributions for mechanical data were less than 15%. The “X” mark indicates that the mechanical test could not be performed because of brittleness. f) The thermotropic properties were measured by differential scanning calorimetry (DSC) (10°Cmin⁻¹) with confirming the softening behavior by crossed polarizing microscopy equipped with a hot-stage, temperature-controlled to $\pm 0.1^\circ$ accuracy. The “N” mark indicates that the transition temperature did not appear. g) The 10% weight loss temperature, T₁₀, was measured by thermogravimetry analysis (TGA) under nitrogen (10°Cmin⁻¹). h) Biodegradation means the degradation in soil plus the hydrolysis to convert into the naturally-occurring molecules. The data in parenthesis were obtained after UV-irradiation for 4 hours (wavelength: >250 nm, strength: 130 mW•cm⁻²). i) The Mn was about 8000, as estimated by the ¹H NMR study.

Figure Captions

Figure 1. Structural analysis and liquid crystalline behavior of poly(4HCA-co-DHCA)s. **a**, chemical structure of the hyperbranch polyarylates. **b**, the representative texture taken at 220 °C by crossed-polarizing microscopy showing the nematic Schlieren texture. **c**, samples processed by pressure above the softening temperature of 230 °C. **d**, a representative wide angle X-ray diffraction (WAXD) image of the copolymer with a C of 45 %. The specimens were prepared by mechanical elongation at 230 °C (inset picture; scale bar 1 cm). The diffraction intensity was shown by a color scale from purple (weak) to red (intense).

Figure 2. Degradation behavior of copolymer samples. **a**, Weight change of non-UV-irradiated pellets of the copolymers with different C values (diameter:10 mm, thickness: 0.5 mm, weight: 50 mg) immersed in a buffer solution of pH=10 at 60 °C. Edges of the error bar show maximum and minimum values of data in two times tests. **b**, Photos of the C=21 copolymer compact buried in soil for 10 months. left: Macroscopic digital image. right: FE-SEM image of the sample surface, showing the local cave-in with a micrometer size (arrows). **c**, Weight change of the copolymer pellets with different C values tested after UV-irradiation for 3 hours. Edges of the error bar show maximum and minimum values of data in two times tests. Sample dimension was the same with **a**. **d**, The hydrolysis mechanism of the copolymers photoconverted to form the cyclobutane group.

Figure 3 Photoreaction of poly(4HCA-co-DHCA)s by ultraviolet (UV)-irradiation at a wavelength (λ) longer than 250 nm (UV intensity: 130 mWcm⁻²). **a, change in the UV absorption spectra of a thin film cast onto glass as a function of the irradiation time. **b**, ¹H NMR spectrum of the UV-irradiated sample. **c**, typical photoreaction scheme of the cinnamic group. **d**, time course of the photoconversion degree estimated by UV-absorption at the maximum.**

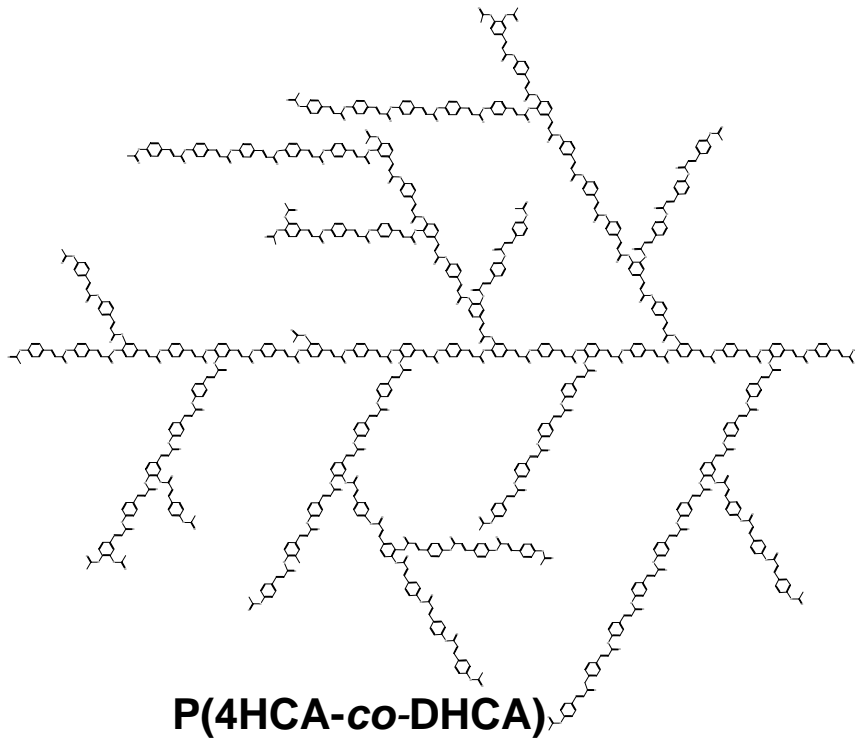
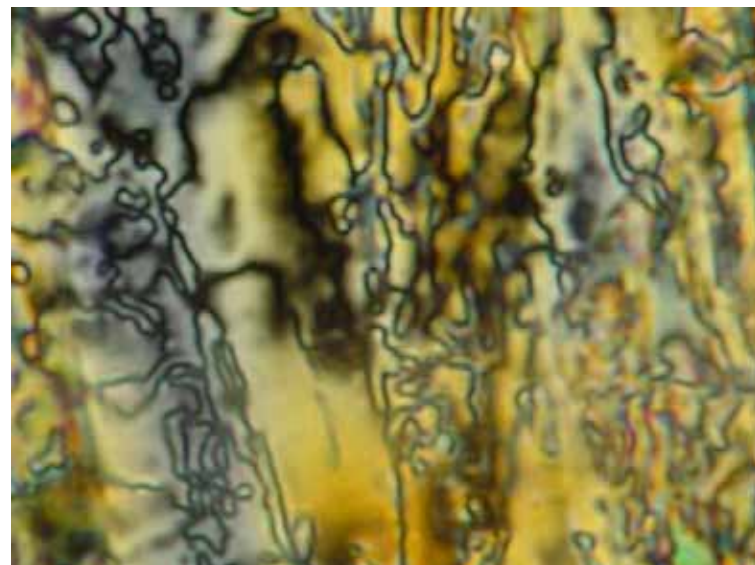
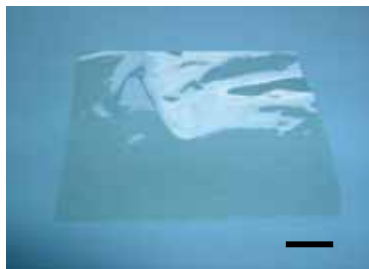
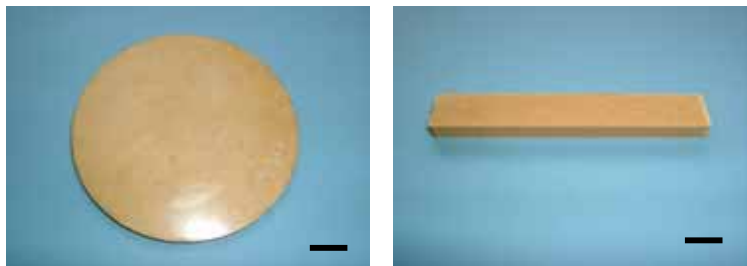
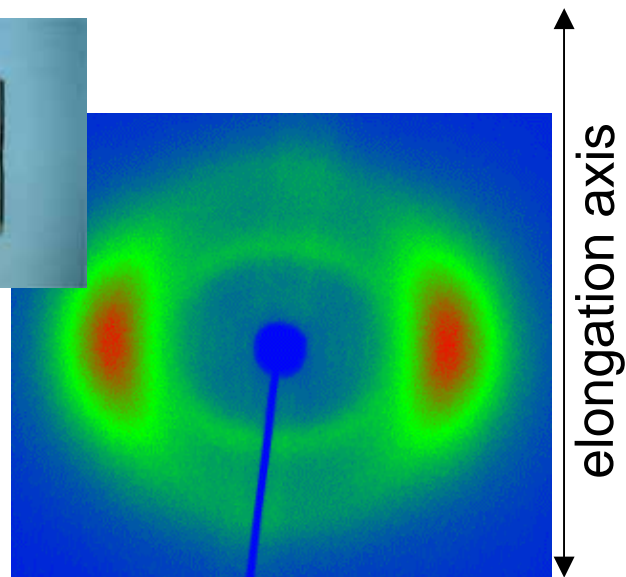
a**b****c****d**

Figure 1 Kaneko et al.

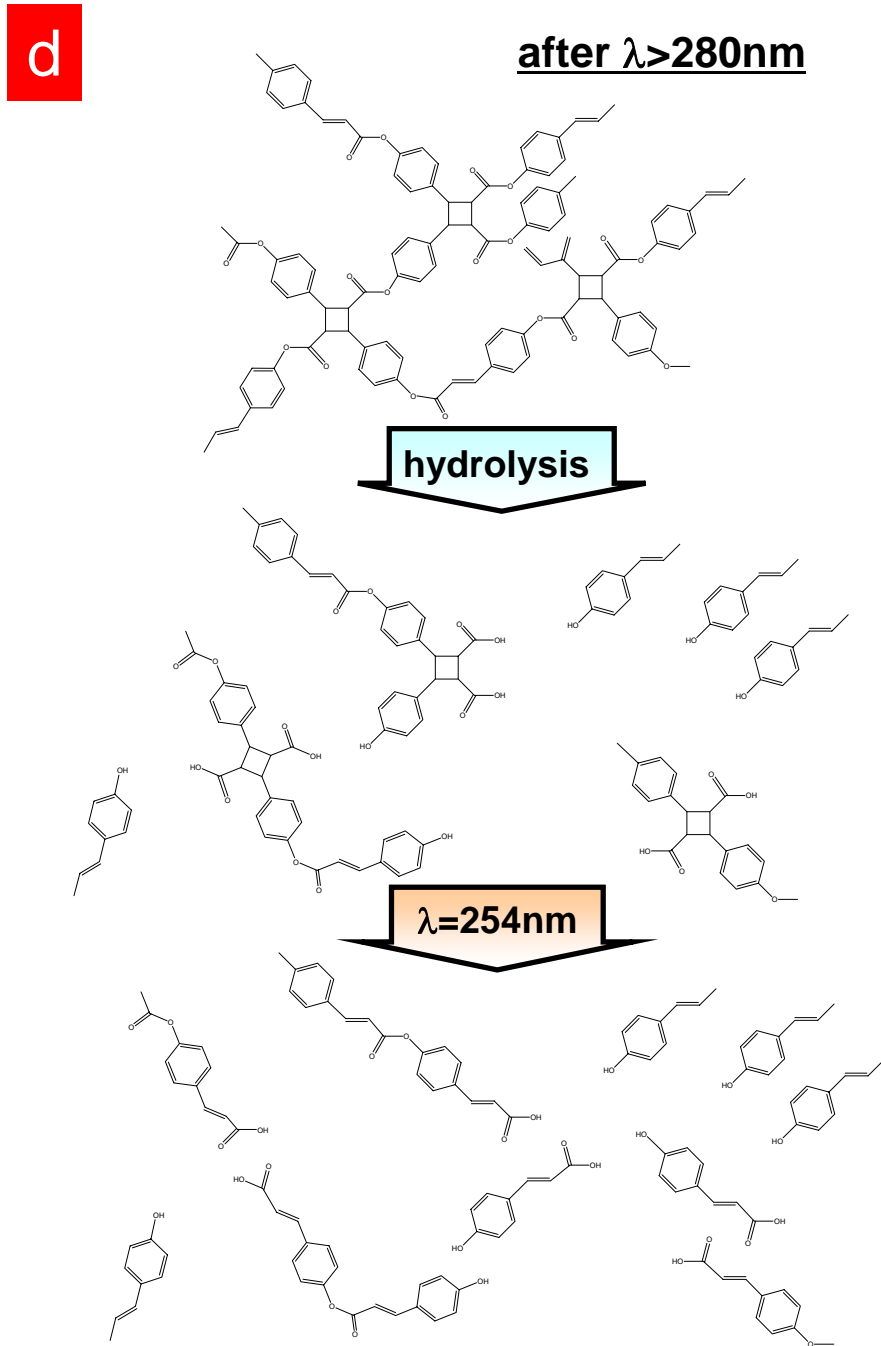
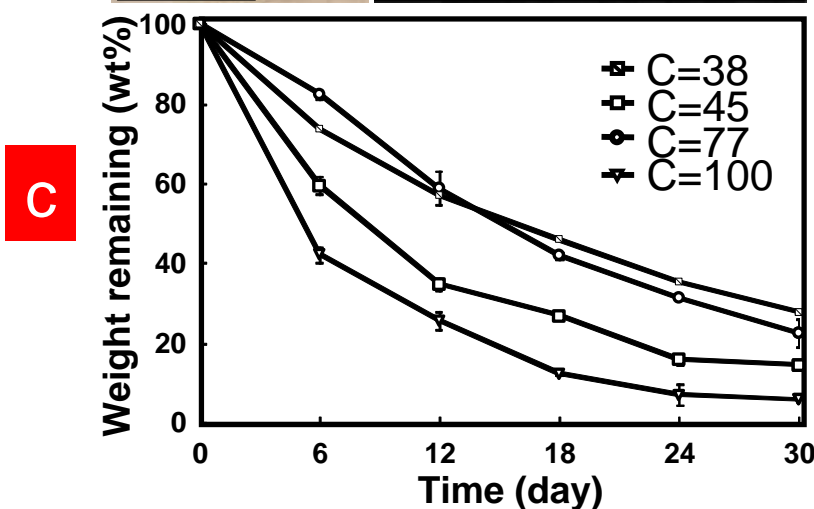
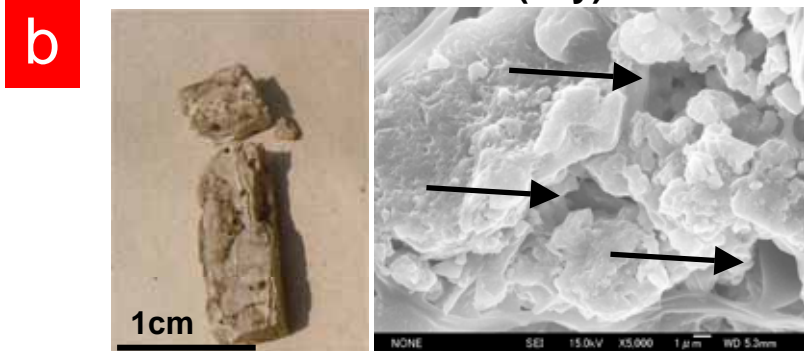
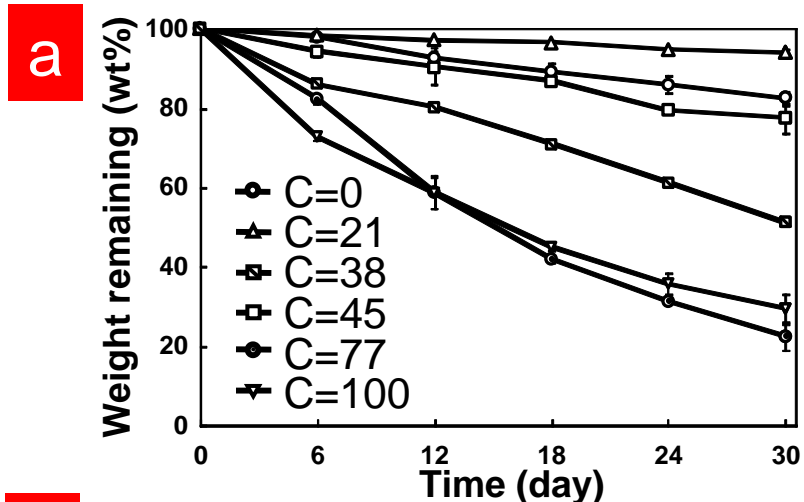


Figure 2 Kaneko et al.

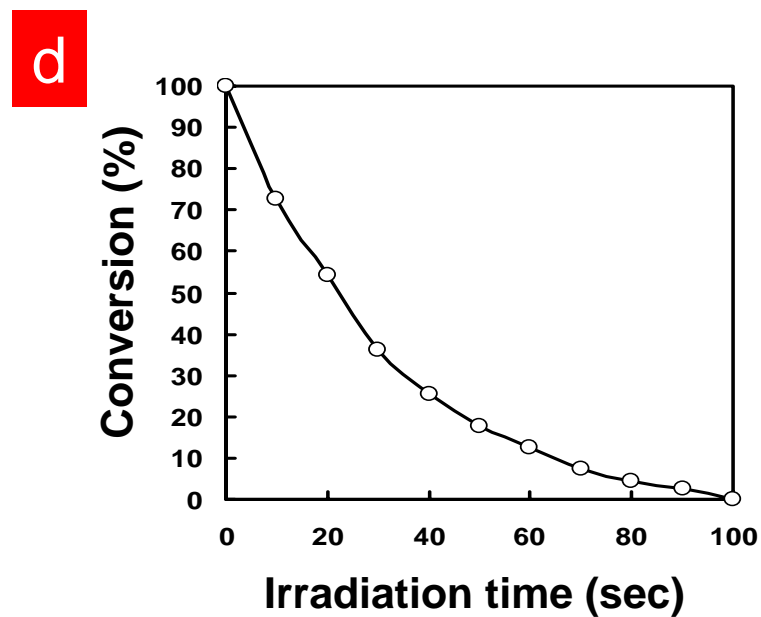
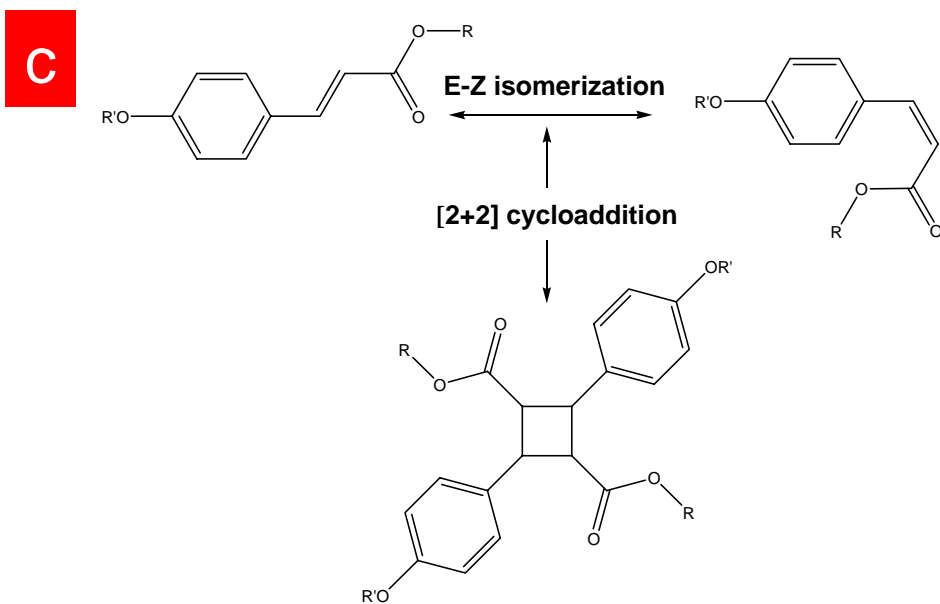
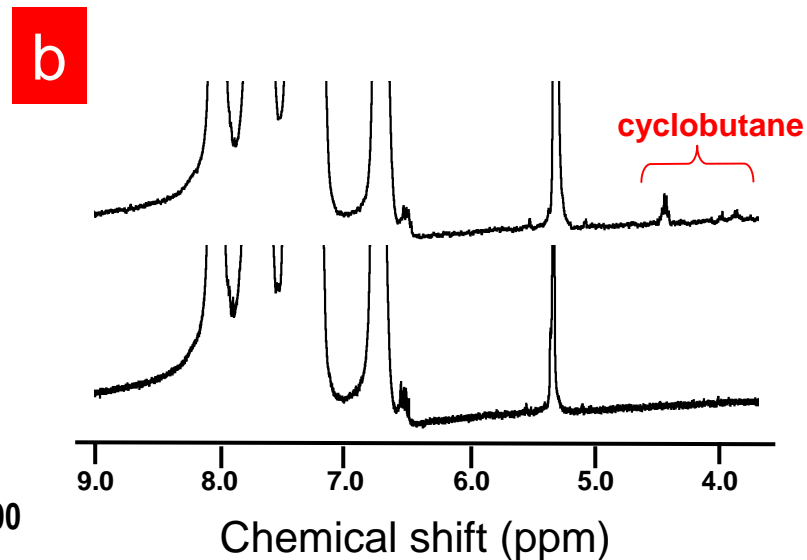
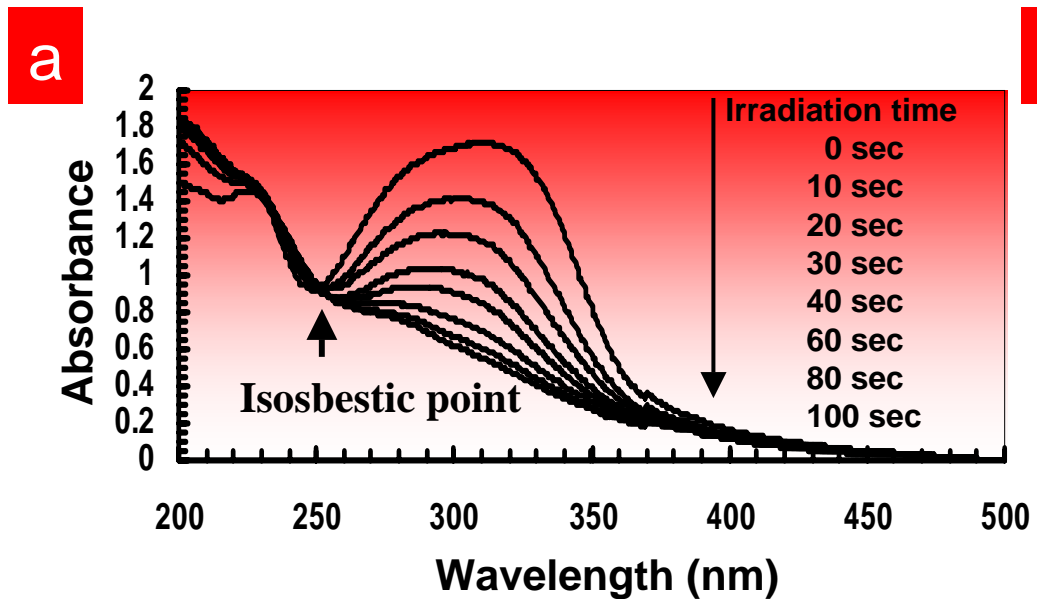


Figure 3 Kaneko et al.